NJC

ROYAL SOCIETY OF CHEMISTRY

PAPER

View Article Online
View Journal | View Issue

Cite this: *New J. Chem.*, 2020, **44**, 21309

1*H*-Benzimidazole-5-carboxamidine derivatives: design, synthesis, molecular docking, DFT and antimicrobial studies†

Meryem Erol, *[a] Ismail Celik,[ab] Ozlem Temiz-Arpaci,[b] Hakan Goker,[b] Fatma Kaynak-Onurdag[c] and Suzan Okten[c]

Received 16th April 2020,
Accepted 18th November 2020

DOI: 10.1039/d0nj01899f

rsc.li/njc

In this study, 15 new *N*-(cyclohexyl)-2-substituted-1*H*-benzimidazole-5-carboxamidine derivatives that could be new antimicrobial agents were synthesized and their antimicrobial activities were determined using the microdilution method. Some of the derivatives showed significant efficacy against MRSA and VREF with an MIC value of 8 μg mL^{-1} compared to reference drugs. Molecular docking studies of the compounds against PBP4 and active and allosteric regions of PBP2a were performed and estimated ADME profiles were calculated. The nitrogens of the amidine group of **M7**, one of the most effective antimicrobial compounds compared to reference drugs, formed two separate hydrogen bonds with ASP275 (1.77 Å) and ASP295 (1.83 Å) in the allosteric region of PBP2a. Geometric optimization parameters, MEP analysis, and HUMO and LUMO quantum parameters of **M7** were calculated using DFT/B3LYP theory and the 6-311G(d,p) basis set and the results are displayed.

1. Introduction

Infectious diseases caused by bacteria and fungi are one of the most important threats to public health. In recent years, there have been serious problems with resistance development and toxicity in the treatment of hospital infections caused by resistant Gram-positive bacteria and opportunistic fungal infections caused by suppression of the immune system for various reasons.[1] In particular, methicillin-resistant *Staphylococcus aureus* (MRSA) and vancomycin-resistant *Enterococcus faecalis* (VREF) infections have increased significantly due to the random use of antibacterial drugs.[2] The mortality rate in infectious diseases is the second most common cause of death due to cardiovascular diseases and antibiotics are the most widely used drugs in the world.[3] Every year, 700 000 people die worldwide due to bacterial infectious diseases that are resistant to antibiotics only. In the prevention or treatment of such infectious diseases, it is estimated that if new remedies cannot be developed, the number of people dying each year will reach 10 million people worldwide by 2050, and this figure will be much higher than the deaths caused by cancer, cardiovascular and neurological diseases.[4] Therefore, the discovery of new and more effective antimicrobial drugs is very important and many studies have been performed to design new agents.

The final stages of cell wall biosynthesis in bacteria are carried out by penicillin-binding proteins (PBPs), which form cross-links in peptidoglycan chains. Since inhibition of these enzymes reduces the structural integrity of the cell wall, beta-lactam is the target of antibiotics. In methicillin-sensitive *S. aureus* (MSSA), there are five PBPs, while a different PBP, called PBP2 or PBP2a, is synthesized in MRSAs.[5] Unlike other PBPs, PBP2/2a shows a low affinity for antibiotics in the β-lactam structure. Therefore, in the presence of β-lactam group antibiotics, it is the only transpeptidase capable of sustaining peptidoglycan synthesis by performing the function of high-affinity PBPs.[6,7] PBPs encode genes called mecA and mecC, and these genes are located on the SCCmec cassettes in the bacterial chromosome. The mechanism of resistance is the synthesis of a new penicillin-binding protein (PBP2a) encoded by the mec-A gene.[8–10] In *E. faecalis*, decreased sensitivity to β-lactam antibiotics is due to the expression of PBP4.[11,12]

The benzimidazole ring system has an important role to play in many pharmacological activities such as antimicrobial,[13–17] antiviral,[18] anthelmintic,[19] antihistamine,[20] antiulcer,[21] antihypertensive,[22] anticancer,[23] antioxidant,[24] spasmolytic,[25] anticonvulsant,[26] anti-inflammatory,[27] antiasthmatic,[28] and analgesic.[29] Therefore, studies on these derivatives have been increased in recent years. Research to date reveals that the benzimidazole ring system is mostly substituted from the 1st,

[a] *Erciyes University, Faculty of Pharmacy, Department of Pharmaceutical Chemistry, Kayseri, Turkey. E-mail: eczacimeryem@gmail.com*
[b] *Ankara University, Faculty of Pharmacy, Department of Pharmaceutical Chemistry, Ankara, Turkey*
[c] *Trakya University, Faculty of Pharmacy, Department of Pharmaceutical Microbiology, Edirne, Turkey*

† Electronic supplementary information (ESI) available. See DOI: 10.1039/d0nj01899f

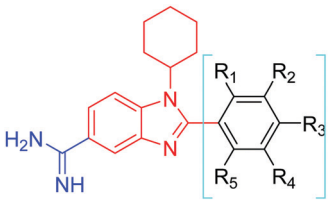

R_1: H, CH_3, OCH_3, benzyloxy
R_2: H, F, COOH
R_3: Cl, Br, CH_3, C_2H_5, OCH_3, COOH, dimethylamino, benzyloxy, phenyl
R_4: H; R_5: H

Fig. 1 Designed 1*H*-benzimidazole-5-carboxamidine derivatives.

2nd, and 5th positions.[30,31] Groups in these positions are generally thought to play a role in their impact and severity. Since this ring system is a structural bioisostere of adenine and guanine structures carrying purine nuclei, it is thought that they can demonstrate their microbiological activities in this way.[32] *In vivo* and *in vitro* activity studies have shown that aromatic amidine and diamidine group compounds have strong activity against a large number of bacteria, amoeba, protozoa, and viruses. The mechanisms of action of this group of compounds are still not fully elucidated, possibly due to their action by more than one mechanism of action. The intensely emphasized mechanism is reported to be that aromatic amidine and diamidine derivatives act by binding to the minor cavity of adenine and thymine-rich DNA and inhibiting one or more DNA-dependent enzymes or inhibiting direct transcription.[33–38] In new drug development studies, it is known that new compounds with a stronger effect can be found with the combination of different groups of pharmacophores in the same molecule. In some studies, microbiological activities of compounds carrying a benzimidazole ring and amidine group against existing bacteria and their isolates were investigated and some derivatives were found to be more effective than standard drugs.[4,39–42]

In light of this information, it was aimed in this study to synthesize some new mono cationic benzimidazole carboxamidine derivatives (Fig. 1), to clarify the structures of the compounds using ^{1}H-NMR, ^{13}C-NMR, mass spectroscopy, and elemental analysis methods and to investigate *in vitro* antimicrobial activities compared to clinical reference drugs. Estimation of ADME profiles of all compounds, molecular docking studies with Schrödinger, molecular mechanics generalized born surface area (MM-GBSA) calculations, and molecular reactivity analyses (HOMO–LUMO) were performed. Also, molecular electrostatic potential (MEP) analysis and geometric optimization of **M7**, which has one of the highest antimicrobial activities *in vitro*, were performed.

2. Experimental

2.1. General procedures for the preparation of compounds (M1–M15)

4-Chloro-3-nitrobenzonitrile (2 g, 10.95 mmol) and cyclohexylamine (2.3 mL, 20 mmol) were reacted at 100 °C for 4–5 hours in the presence of 6 mL of DMF. The reaction medium was cooled, water was added and precipitated, the product was crystallized from ethylacetate-*n*-hexane (50 : 50) and compound **1** was obtained.[39,43,44] Absolute EtOH was treated with dry HCl gas for about 40–45 minutes (Pinner reaction). Acid-ethanol (6–7 mL) was added to compound **1** (10 mmol) until the product dissolved and was left to stir at room temperature for 5–6 days. At the end of the period, it was diluted with dry ether, filtered under vacuum, and dried at room temperature (compound **2**). The imidate esters (5 mmol) were left to stir for 2–3 days at room temperature with ammonia gas (6–7 mL) passed through EtOH. At the end of the period, some of the EtOH was evaporated, diluted with ether, allowed to be vacuum filtered and dried (compound **3**).[45] Amidine (0.75–0.80 g) was subjected to a reduction in ethanol with 40 mg of a 10% Pd–C catalyst. The resulting product was obtained by filtering through a Celite bed (compound **4**).[43,46,47] The relevant aldehyde derivatives (15 mmol) that provided the cyclization of the benzimidazole ring were dissolved in 50 mL of EtOH. A solution of 1.6 g $Na_2S_2O_5$ in 10 mL of water was added slowly over the aldehyde solution. The reaction mixture was shaken vigorously and more EtOH was added. The mixture was kept in the refrigerator for a few hours, and the precipitate was filtered off and dried.[48] The targeted result products were obtained by reacting aldehyde salts and compound **4** in DMF for 6 hours at 100 °C.[49,50] At the end of the period, the reaction medium was precipitated with Na_2CO_3 solution and filtered. A portion of the resulting crude product was purified by column chromatography using a chloromethane : methanol : ammonia (10 : 1 : 0.1) solvation mixture, while the other was crystallized from methanol. In the last step, the HCl salts of the compounds were obtained from HCl gas-passed EtOH.[72] The intermediate products (compound **1**, **2**, **3**, and **4**) are not original.[51] A list of the synthesized compounds (Table S1, ESI†) and their physical and spectral data are reported in the ESI.†

2.2. Antimicrobial activity

2.2.1. Microorganisms and standard drugs. *Escherichia coli* ATCC 25922, *Pseudomonas aeruginosa* ATCC 27853, *Staphylococcus aureus* ATCC 29213, *Enterococcus faecalis* ATCC 29212, and *Candida albicans* ATCC 10231 standard strains and clinical isolates provided from Trakya University Health Center for Medical Research and Practice (Hospital) were used in the study. Ampicillin (Sigma), vancomycin (Sigma), ciprofloxacin (Sigma), meropenem (Sigma), gentamycin (Sigma), and amphotericin B (Sigma) were used as standard antimicrobial agents.

2.2.2. Microdilution method. Stock solutions of the test compounds were prepared in DMSO (Merck). Mueller Hinton Agar (MHA) (Merck), Mueller Hinton Broth (MHB) (Merck), Sabouraud Dextrose Agar (SDA) (Merck), Sabouraud Liquid Medium (SLM) (Merck), and RPMI-1640 medium (Sigma) with L-glutamine buffered with 3-[*N*-morpholino]-propansulfonic acid (MOPS) (Sigma) (pH: 7) were used in the study. Susceptibility testing was performed according to the guidelines of the Clinical and Laboratory Standards Institute (CLSI) M100-S25[52] and M27-A3.[53] 100 μL of MHB and RPMI-1640 medium with

L-glutamine (Sigma) buffered with MOPS (pH: 7) were added to each well of the microplates for bacteria and fungi, respectively. The bacterial suspensions used for inoculation were prepared at 10^5 CFU mL^{-1} by diluting fresh cultures at McFarland 0.5 density. Suspensions of the yeast at McFarland density were diluted 1 : 100 and 1 : 20 respectively and 2.5×10^3 CFU mL^{-1} were inoculated to the twofold-diluted solution of the compounds. Stock solutions of the tested compounds and standard drugs were diluted two-fold in the wells of the microplates so the solution of the synthesized compounds was prepared at 512, 256, 128, 64, 32, 16, 8, and 4 μg mL^{-1}, and standard drugs were prepared at 16, 8, 4, 2, 1, 0.5, 0.25, and 0.125 μg mL^{-1} concentrations. All solvents and diluents, pure microorganisms, and pure media were used in control wells. A 10 μL microorganism inoculum was added to each well of the microplates. Microplates including bacteria were incubated at 37 °C for 16–20 h and microplates including fungi were incubated at 35 °C for 24–48 h. After incubation, the lowest concentration of the compounds that completely inhibits macroscopic growth was determined and reported as the minimum inhibitory concentration (MIC). All organisms were tested in triplicate in each run of the experiments. Solvents, pure microorganisms, and pure media were used as control wells.

2.3. Molecular docking studies

The molecular docking study was carried out using the Maestro 11.5 program (Schrodinger Inc. USA)[54] in 5 stages: protein preparation, ligand preparation, grid box creation, displaying docking, and docking results. The crystal structure of *S. aureus* PBP2a in complex with Quinazolinone (PDB ID: 4CJN at 1.95 Å resolution),[55,56] and crystal structure of *E. faecalis* PBP4 in the ceftaroline-bound form (PDB ID: 6MKI at 2.98 Å resolution)[11] were imported from the protein data bank (https://www.rcsb.org/). Ligands were minimized using 'LigPrep' and prepared with the OPLS3 force field with possible ionizations at pH = 7 ± 2. 'Protein Preparation Wizard' was used for the protein structures: preprocess, the removal of water and other molecules was minimized after optimizing using PROKA pH: 7.0. 'Receptor Grid Generation' was used for the binding site: for the 4CJN allosteric site *x*: 45.05, *y*: 44.42 and *z*: 7.36 coordinates, for the 4CJN active site *x*: −35.89, *y*: −12.57 and *z*: −23.65 coordinates and for the 6MKI active site *x*: 35.24, *y*: 1.34 and *z*: 10.06 coordinates were created in 20 × 20 × 20 Å. Ligands and proteins prepared for the binding site determined using 'Ligand Docking' were docked using Extra Precision (XP). MM-GBSA values were calculated according to the obtained docking poses.[57]

2.4. MM-GBSA free energy calculations

MM-GBSA is a popular approach used to estimate protein–ligand free energies. It allows us to examine whether key interactions are established and stabilized during molecular dynamics simulation. The stability of the binding is determined by subtracting the hollow protein and single ligand energies from the total energy of the protein–ligand complex. $\Delta G_{bind} = E_{complex}$ (minimized) − [E_{ligand} (unbound, minimized) + $E_{receptor}$ (unbound, minimized)] is calculated with the formula. Calculations were made using the Schrödinger Prime module.[58,59]

2.5. DFT/B3LYP calculations

Quantum chemical calculations of the compounds were carried out using the Gaussian 09 package program[60] and DFT/B3LYP theory and the 6-311G(d,p) basis set.[61–68] HOMO–LUMO energies of all compounds and other electronic parameters calculated from these energies (ionization potential, electron affinity, electronegativity, chemical hardness, chemical softness, chemical potential, and electrophilic index, *etc.*) were calculated. Also, the molecular electrostatic potential (MEP) and optimized geometrical structure results of M7, which is one of the compounds showing the best antimicrobial activity, were theoretically obtained. First, the **M7** was optimized to find its minimum energy and its most stable structure. The results are shown using the GaussView 6 program.[69]

2.6. Theoretical ADME predictions

One of the biggest problems of drug design is that compounds with strong biological effects also do not have good pharmacokinetic effects.[70] Therefore, for the evaluation of the absorption, distribution, metabolism, and elimination profiles of the synthesized compounds, physicochemical parameters such as log *P*, PSA, nrotb, % human oral absorption, molecular weight, and number of hydrogen bond donor–acceptor were calculated using Schrodinger Maestro's QikProp program.[71]

3. Results and discussion

3.1. Chemistry

M1–M15 was synthesized using the methods given in the Experimental section and shown in Scheme 1. After the purity controls of the synthesized compounds (TLC studies) and their melting points were determined, spectral analyses were performed to prove the structures. ^{1}H-NMR, ^{13}C-NMR, Mass spectral analysis, and elemental analysis were found to prove the expected structures. First, the reaction product of 4-chloro-3-nitrobenzonitrile and cyclohexylamine in the presence of DMF was used to prepare **1**. Subsequently, compound **2** was formed by the Pinner reaction method. The resulting unstable imidate esters were rapidly converted to compound **3** with NH_3/EtOH, followed by reduction of the nitro group on the Pd/C catalyst with hydrogen gas to obtain compound **4**, and then **M1–15** was obtained in the presence of aldehyde salts and DMF. HCl salts of the compounds were obtained from HCl gas-passed EtOH.

In the resulting compounds, aromatic protons were between 6.85–8.35 ppm and cyclohexyl protons were between 1.14–4.42 ppm (protons are not separated). Amidine group protons in some spectra as a wide 4H singlet between 9.08 and 9.36 ppm, and in some spectra as 2H and 2H singlet peaks, were observed, but in some spectra could not be observed due to paramagnetic shift. In mass spectral analysis of the compounds, the ion formed as a result of the breaking of the M + H ion or cyclohexyl group was monitored at 100% relative densities. Elemental analyses of

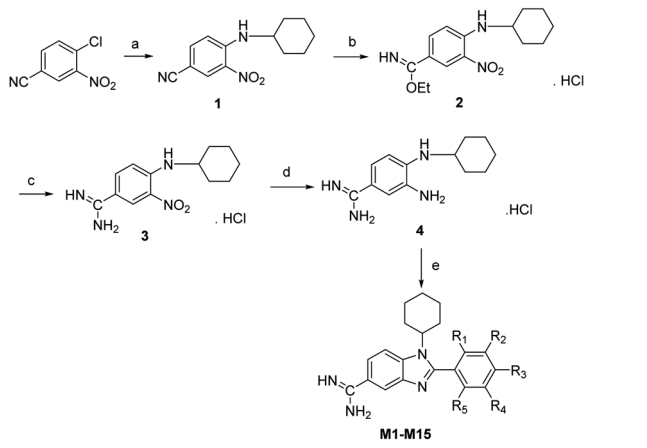

Reagents: a) cyclohexylamine b) HCl(g)/EtOH c) NH_3 /EtOH d) H_2/Pd.C e) $Na_2S_2O_5$ adduct of benzaldehydes

Scheme 1 Synthesis pathways of the target compounds.

the compounds were compared with theoretical calculations to determine the purity of the compounds and the number of other components. The results of the elemental analysis and all spectral data were fully compatible with the molecules presented.

3.2. *In vitro* antimicrobial activities

All synthesized compounds **M1–M15** were tested for *in vitro* antibacterial and antifungal activity against standard strains and drug-resistant isolates. It was carried out according to the broth microdilution technique described by CLSI. The MIC of each compound was determined and compared with ampicillin, gentamycin, vancomycin, meropenem, ciprofloxacin, and amphotericin B. According to microbiological results, the compounds showed an average activity against *E. coli* ATCC 25922 and multi-drug resistant *E. coli* (MIC: 16–256 μg mL^{-1}), while **M8** exhibited the best activity against both strains (MIC: 16 ug mL^{-1}). Even if **M8** did not show more activity than reference drugs, it may be a lead compound to develop new molecules against *E.coli*. The compounds generally had a weak antimicrobial effect against Gram-negative *P. aeruginosa* ATCC 27853 and *P. aeruginosa* isolate (MIC: 64–128 μg mL^{-1}). While half of the compounds against *S. aureus* ATCC 29123 showed good activity with MIC: 8 μg mL^{-1}, they showed weaker efficacy compared to reference drugs. The results of the **M4**, **M7**, **M8**, and **M12** derivatives against MRSA (MIC: 8 μg mL^{-1}) are quite satisfactory compared to ampicillin and meropenem. The compounds showed a broad range of activity against the Gram-positive bacterium *E. faecalis* ATCC 29212 (MIC: 8–512 μg mL^{-1}) compared to the reference drugs. **M7**, **M8**, and **M12** derivatives against VREF showed better efficacy than vancomycin and ampicillin with MIC: 8 μg mL^{-1}. The antifungal activities of the compounds against *C. albicans* were in the range of 8 to >512 μg mL^{-1} and much less effective than amphotericin B.

When the microbiology findings were evaluated in general, it was found that the tested derivatives showed more important antimicrobial activity against Gram-positives than Gram-negatives, and the best antibacterial activity was observed against MRSA and VREF. Benzimidazole does not have a positive effect on the activity of the presence of groups (such as methyl, ethyl) that give electrons to the ring on the phenyl ring at position 2; instead, it has been found to increase antimicrobial activity by substituting it with electron attracting groups such as chlorine, bromine, carboxy, and benzyloxy (Table 1).

Table 1 *In vitro* antimicrobial MIC values (μg mL^{-1}) of the synthesized compounds (**M1–M15**) and reference drugs

Compound	A	B	C	D	E	F	G	H	I
M1	128	128	128	128	16	32	64	64	64
M2	128	128	128	128	8	16	32	32	32
M3	32	32	128	128	8	16	32	32	128
M4	128	128	64	64	8	**8**	16	16	16
M5	128	128	64	512	512	512	512	512	512
M6	64	64	64	64	32	64	32	64	128
M7	128	128	64	64	8	**8**	8	**8**	8
M8	16	16	64	64	8	**8**	8	**8**	>512
M9	128	256	64	64	128	256	128	128	128
M10	128	128	64	64	256	256	128	128	128
M11	128	128	64	64	16	32	64	64	64
M12	32	32	128	128	8	**8**	8	**8**	64
M13	128	128	64	64	8	16	64	64	16
M14	128	128	128	128	128	128	128	128	128
M15	32	32	128	128	32	64	64	64	128
Vancomycin	—	—	—	—	<0.0625	<0.0625	<0.0625	>**8**	—
Ampicillin	2	2	—	—	2	>**8**	2	>**8**	—
Meropenem	<0.0625	<0.0625	0.5	0.5	<0.0625	>**8**	—	—	—
Ciprofloxacin	<0.0625	<0.0625	1	2	0.5	0.5	2	2	—
Gentamicin	0.25	0.25	0.5	>8	1	2	—	—	—
AmphotericinB	—	—	—	—	—	—	—	—	0.5

A: *E.coli* ATCC 25922, B: *E. coli* isolate, C: *P. aeruginosa* ATCC 27853, D: *P. aeruginosa* isolate, E: *S. aureus* ATCC 29213, F: *S. aureus* isolate (MRSA), G: *E. faecalis* ATCC 29212, H: *E. faecalis* isolate (VREF), I: *C. albicans* ATCC 10231. *E. coli* isolate is susceptible to the tested antimicrobial agents. *S. aureus* isolate is a methicillin resistance (MRSA) isolate. Antibacterial drugs are not tested against fungi, while antifungal drugs are not tested against bacteria. *P. aeruginosa* is naturally resistant to ampicillin. Gram (−) bacteria used in this study are resistant to vancomycin.

3.3. Molecular docking

While the synthesized derivatives have a lower effect compared to reference drugs against *S. aureus* and *E. faecalis*, we were focused on the resistance proteins of these strains as they exhibit higher activity against MRSA and VREF. As mentioned in the introduction, it was concluded that the proteins act on PBP2a (PDB: 4CJN) and PBP4 (PDB: 6MKI). Docking studies suggest that the compounds may have been linked by binding to the 4CJN allosteric site. The Glide emodel scores of the docking studies performed in the 4CJN allosteric site generally were calculated to be lower than the active site. One of the most effective antimicrobial compounds, **M7**, formed 1.77 Å and 1.83 Å length hydrogen bonds between the two separate nitrogens of the amidine group and the ASP275 and ASP295 in the 4CJN allosteric site. **M7** showed hydrophobic interactions with GLY296, TYR297, LYS148, ASN146, GLU145, and ILE144. The 2D and 3D interaction diagram of **M7** in the allosteric site of PBP2a (PDB: 4CJN) is given in Fig. 2.

In the 6MKI binding site, **M7** formed a single nitrogen of the amidine group and two separate hydrogen bonds between GLU624 and GLU635 with a length of 1.84 Å. It showed hydrophobic interactions with THR622, GLY621, THR620, VAL467, SER482, ASN484, THR665, and SER663. The reference drug ampicillin formed hydrogen bonding with ASP666, SER482, THR620 and THR622, and hydrophobic interactions with SER663, THR665, GLY621, SER637, TYR605, VAL666 and

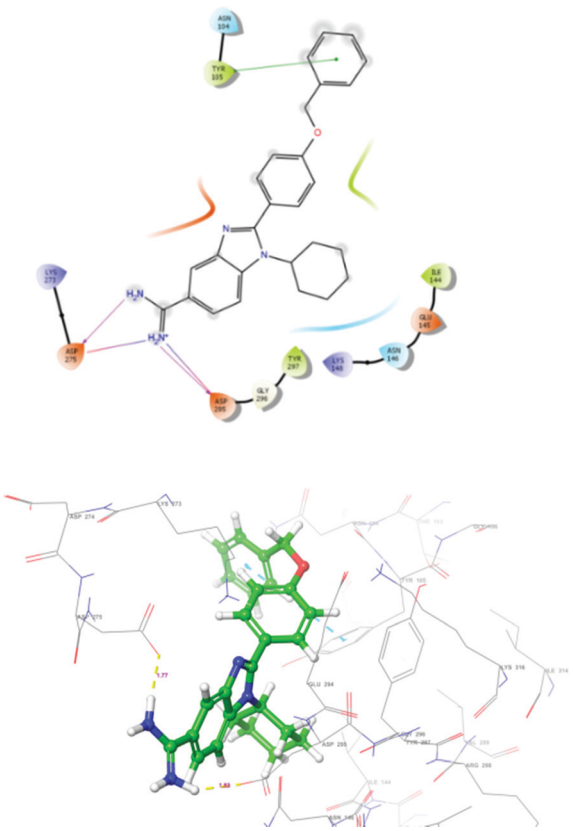

Fig. 2 2D and 3D interaction between **M7** with PBP2a (4CJN) at the allosteric site.

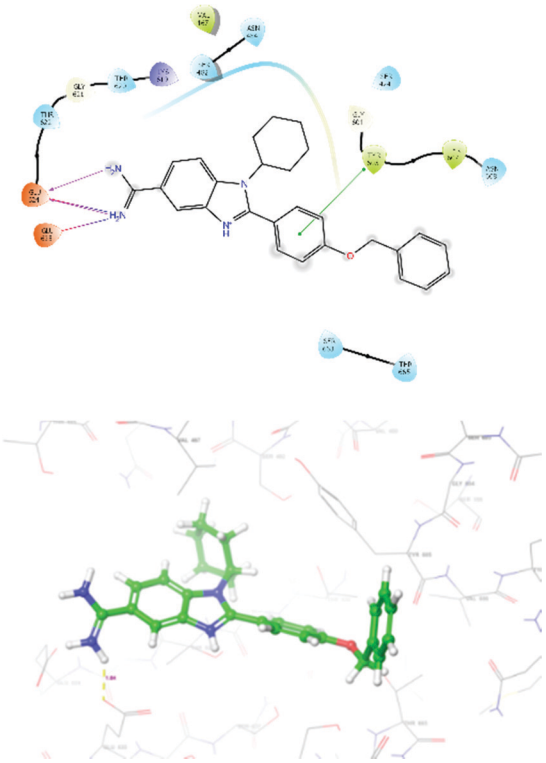

Fig. 3 2D and 3D interaction between **M7** with PBP4 (6MKI) at the active site.

TYR607 (see also ESI†). Fig. 3 shows 2D and 3D interactions of the **M7**'s 6MKI active site.

The amidine group is required for hydrogen bond formation. Hydrogen bonding with GLU624 in the 6MKI active site is important, and the amidine group in the compound framework formed hydrogen bonding with GLU624. Glide emodel, MM-GBSA (dG Bind), and XP Gscore scores of all compounds are given in Table 2. Accordingly, while there was a good correlation between Glide emodel scores and antimicrobial effect, there was a weak relationship between MM-GBSA (dG Bind) and XP Gscore scores.

3.4. Molecular reactivity analyses

Boundary orbitals in the molecule are named as HOMO and LUMO. HOMO is the 'Highest Occupied Molecular Orbital' in a molecule. LUMO, on the other hand, can be defined as the 'Lowest Unoccupied Molecular Orbital' in a molecule. These orbitals describe intermolecular interactions. The energy difference between the HOMO and LUMO orbitals is a measure of the chemical stability of the molecules and plays a major role in determining the chemical and spectroscopic properties of the molecules.[73] Also, molecular properties such as ionization potential (IP), electron affinity (EA), electronegativity (X), chemical hardness (η), chemical softness (S), chemical potential (μ), and electrophilic index (ω) could be determined using this energy range.[74–76] The HOMO–LUMO energies are given in Table 3 and other electronic properties are given Table S2 (ESI†). Fig. 4 shows the regions where **M7**'s HOMO

Table 2 Calculated Glide emodel, MM-GBSA (dG Bind), and XP Gscore values of the compounds and reference drugs

	4CJN						6MKI		
	Allosteric site			Active site			Active site		
Compound	Glide emodel	MM-GBSA	XP Gscore	Glide emodel	MM-GBSA	XP Gscore	Glide emodel	MM-GBSA	XP Gscore
M1	−33.96	−47.25	−3.78	−37.20	−28.53	−4.02	−46.30	−63.20	−7.56
M2	−29.91	−45.20	−4.20	−29.63	−40.29	−4.42	−49.52	−65.37	−7.83
M3	−30.49	−33.80	−2.26	−23.96	−29.50	−5.63	−49.46	−60.55	−7.60
M4	−35.28	−39.53	−1.21	−29.14	−31.68	0.19	−52.06	−61.33	−7.33
M5	−35.54	−38.83	−4.40	−28.13	−33.19	0.02	−50.57	−63.40	−7.46
M6	−32.09	−33.05	−2.77	−23.37	−36.64	−3.94	−44.039	−51.10	−4.39
M7	**−46.28**	−41.28	−3.22	−32.89	**−41.49**	−3.87	**−60.38**	−61.70	−6.53
M8	−37.34	−36.62	−2.71	−3.54	−19.45	−2.29	−55.45	−56.67	−4.28
M9	−41.41	−29.65	−3.00	−29.67	−19.27	−4.78	−46.49	−38.83	−7.21
M10	−39.69	−40.17	−4.22	−37.21	−27.49	−4.71	−55.83	−41.43	−8.44
M11	−39.69	−40.17	−4.22	−36.85	−38.15	−3.06	−44.96	−58.49	−4.99
M12	−43.39	−39.30	−3.58	−50.60	−50.30	−4.52	−55.40	−62.24	−4.97
M13	−43.39	−39.30	−3.58	−25.21	−47.39	−4.20	−46.75	−65.17	−7.59
M14	−30.26	−42.51	−3.02	−39.57	−38.98	−2.42	−46.76	−59.89	−7.38
M15	−37.98	−38.63	−3.90	−32.86	−31.40	−4.63	−50.91	−59.36	−7.81
Vancomycin	−75.60	−57.85	−6.23	−70.03	−30.43	−5.48	−70.73	−95.36	−6.77
Ampicillin	−36.56	−27.08	−3.58	−32.24	−32.61	−3.71	−43.25	−25.30	−4.93
Gentamycin	−31.87	−40.88	−3.41	28.64	−17.92	−2.18	−77.75	−68.84	−2.08
Meropenem	−40.45	−44.19	−4.55	−37.23	−32.54	−6.47	−48.57	−46.11	−5.18
Ciprofloxacin	−32.61	−37.05	−2.67	−47.96	−54.78	−5.99	−46.66	−52.33	−5.21

Table 3 Calculated HOMO–LUMO energy values of **M1–M15**

Compound	HOMO	LUMO	ΔE
M1	−0.20910	−0.04849	0.16061
M2	−0.20827	−0.04766	0.16061
M3	−0.20508	−0.04260	0.16248
M4	−0.21955	−0.05577	0.16378
M5	−0.21066	−0.05722	0.15344
M6	−0.18287	−0.02934	0.15353
M7	**−0.21133**	**−0.03620**	**0.17513**
M8	−0.20563	−0.06337	0.14226
M9	−0.21330	−0.07899	0.13431
M10	−0.21256	−0.06870	0.14386
M11	−0.20803	−0.04758	0.16045
M12	−0.19774	−0.04087	0.15687
M13	−0.20220	−0.04392	0.15828
M14	−0.20696	−0.05216	0.1548
M15	−0.21853	−0.05794	0.16059

and LUMO orbitals are localized. A moderate relationship can be established between the HOMO–LUMO values of the compounds and their antimicrobial effects against MRSA and VREF. One of the most active compounds against both MRSA and VREF, **M7**, has the highest quantum parameters with HOMO = −0.21133, LUMO = −0.03620 and ΔE = 0.17513.

3.5. MEP analysis

MEP is a method that allows us to understand the molecular polarity while correlating the electronegativity, charge, dipole moment, and chemical reaction rate of a compound and also provides information about the net electrostatic effect created by the total charge. An MEP energy map was used to identify regions where the electron density of **M7** is located and thus to predict the reactive regions of electrophilic and nucleophilic attacks. The importance of MEP is also that molecules show both size and shape as well as positive, negative, and neutral electrostatic potential regions. It also provides important information about the formation of intramolecular hydrogen bonds. Potential increases are listed as red < orange < yellow < green < blue.[77] While the red color is related to the regions where the electrons are dense, the blue color represents the electropositive points. Fig. 5 shows the MEP map of **M7**. When the MEP map of **M7** is examined, the electrophilic regions are around the N atom and the nucleophilic regions are around the C and H atoms. The hydrogen bonding of the amidine group of **M7** with ASP275, ASP295, GLU624, and GLU635 in the PBP4 and PBP2a binding sites shows that the molecular docking results are consistent with MEP analysis.

3.6. Geometry optimization

The geometry of the molecule is of great importance in the theoretical calculations of molecular energy and other properties. Even small changes in molecular geometry affect the energy of the molecule. Geometry optimization is the optimization step in which the geometry of the molecular system has the lowest energy corresponding to the base state by changing the geometric parameters (bond length, bond angles, and dihedral angle) of the structure. When the molecules are most stable, they also correspond to atomic sequences where their energy is minimal. The experimental geometric structure of the compounds is unknown.[78] In some recent studies, experimental and computational studies of the molecular geometry of compounds have been reported as comparisons.[79,80] The numbered optimized geometrical structure of **M7** is given in Fig. 6.

3.7. Theoretical ADME prediction

Oral bioavailability studies of the compounds (absorption, distribution, metabolism, and elimination) are essential to eliminate compounds with unacceptable pharmacokinetic properties and for successful drug discovery studies. *In silico*

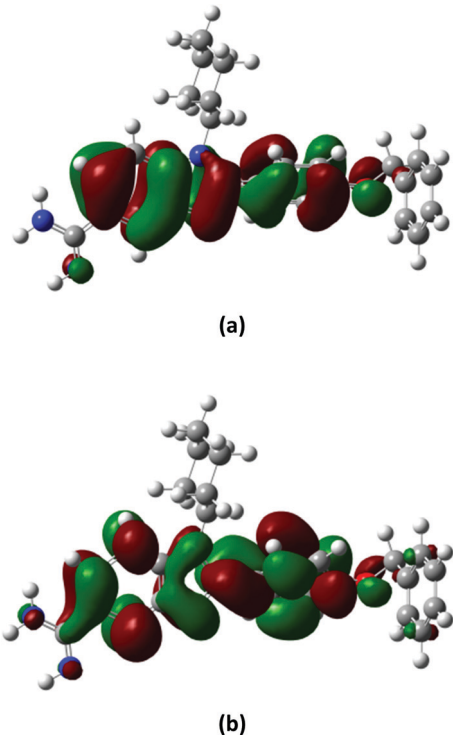

Fig. 4 (a) HOMO and (b) LUMO plots of **M7**.

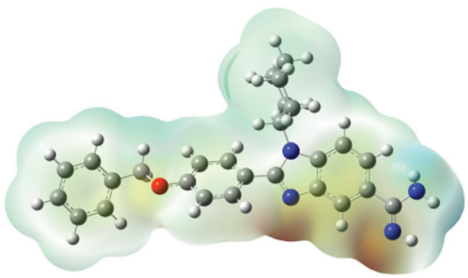

Fig. 5 MEP map of **M7**.

ADME and toxicological screening systems can provide an opportunity to predict performance *in vivo*. Estimates of ADME properties of all synthesized compounds (**M1–M15**) were performed with QikProp. This software evaluates drug candidates' ADME profiles according to Lipinski's five rules and Jorgensen's three rules, and there should be no more than one violation of drug-like compounds. Software data such as molecular weight, log *P*, polar surface area, hydrogen donor number, hydrogen acceptor number, rotatable bond number, and volume are presented in Table S3 (ESI†) with violations of the third and fifth rules. From the table, it can be seen that all the compounds comply with these rules. This increases the probability that the compounds are potential drug molecules.

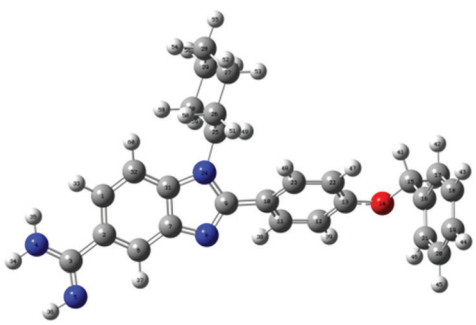

Fig. 6 Optimized molecular structure of **M7**.

4. Conclusions

In this study, a series of *N*-(cyclohexyl)-2-substituted-1*H*-benzimidazole-5-carboxamidine derivatives, which we hope may be a new antimicrobial agent, were designed and synthesized and their antimicrobial activity was determined. **M7**, **M8**, and **M12** derivatives have been observed more effectively compared to reference drugs against both MRSA and VREF, with an MIC value of 8 μg mL^{-1}. Derivatives show more antibacterial activity against Gram-positive than Gram-negative; in particular, binding of groups attracting electrons to the phenyl ring has been observed to significantly increase the antimicrobial activity. For one of the most effective antimicrobial compounds, **M7**, 2D/3D interactions were displayed in the 4CJN active and allosteric site and 6MKI active site, and DFT calculations were performed to estimate its geometric structure and electronic properties. The nitrogens of the amidine group made two separate hydrogen bonds in both sites, and when the scores of all compounds were examined, a good relationship was found between Glide emodel scores and antimicrobial effect. According to all these results, the synthesized compounds showed promising antimicrobial activity.

Conflicts of interest

There are no conflicts to declare.

Acknowledgements

NMR, mass spectra, and elemental analysis of the compounds were performed by Ankara University Faculty of Pharmacy Central Laboratory and Erciyes University Technology and Research Center (TAUM). This work was supported by The Scientific and Technological Research Council of Turkey (TUBITAK) Grant [315S333].

Notes and references

1 J. M. Blair, M. A. Webber, A. J. Baylay, D. O. Ogbolu and L. J. Piddock, *Nat. Rev. Microbiol.*, 2015, **13**, 42–51.
2 H. W. Boucher, G. H. Talbot, J. S. Bradley, J. E. Edwards, D. Gilbert, L. B. Rice, M. Scheld, B. Spellberg and J. Bartlett, *Clin. Infect. Dis.*, 2009, **48**, 1–12.
3 W. Kaplan and R. Laing, *Priority medicines for Europe and the world*, World Health Organization, Geneva, 2004.
4 K. U. Jansen, C. Knirsch and A. S. Anderson, *Nat. Med.*, 2018, **24**, 10–19.

5 C. J. Hackbarth and H. F. Chambers, *Antimicrob. Agents Chemother.*, 1993, **37**, 1144–1149.
6 R. J. Gordon and F. D. Lowy, *Clin. Infect. Dis.*, 2008, **46**, S350–S359.
7 B. L. de Jonge and A. Tomasz, *Antimicrob. Agents Chemother.*, 1993, **37**, 342–346.
8 P. Appelbaum, *Clin. Microbiol. Infect.*, 2006, **12**, 3–10.
9 P. C. Appelbaum, *Clin. Infect. Dis.*, 2007, **45**, S165–S170.
10 A. C. Shore, E. C. Deasy, P. Slickers, G. Brennan, B. O'Connell, S. Monecke, R. Ehricht and D. C. Coleman, *Antimicrob. Agents Chemother.*, 2011, **55**, 3765–3773.
11 T. M. Moon, É. D. D'Andréa, C. W. Lee, A. Soares, J. Jakoncic, C. Desbonnet, M. Garcia-Solache, L. B. Rice, R. Page and W. Peti, *J. Biol. Chem.*, 2018, **293**, 18574–18584.
12 L. B. Rice, C. Desbonnet, A. Tait-Kamradt, M. Garcia-Solache, J. Lonks, T. M. Moon, É. D. D'Andréa, R. Page and W. Peti, *mBio*, 2018, **9**, e00361–e00318.
13 M. Abdel-Motaal, K. Almohawes and M. A. Tantawy, *Bioorg. Chem.*, 2020, 103972.
14 A. Kumar, Y. Kumar, J. K. Sahu and S. Kumar, *Curr. Drug Discovery Technol.*, 2020, **17**, 87–91.
15 M. M. Morcoss, M. El Shimaa, R. A. Ibrahem, H. M. Abdel-Rahman, M. Abdel-Aziz and D. A. Abou El-Ella, *Bioorg. Chem.*, 2020, 103956.
16 S. Harer, M. Bhatia and V. Kawade, *Med. Chem.*, 2019, **15**, 813–832.
17 Y. Bansal, M. Kaur and G. Bansal, *Mini-Rev. Med. Chem.*, 2019, **19**, 624–646.
18 A. Kanwal, M. Ahmad, S. Aslam, S. A. R. Naqvi and M. J. Saif, *Pharm. Chem. J.*, 2019, **53**, 179–187.
19 P. Sethi, Y. Bansal and G. Bansal, *Med. Chem. Res.*, 2018, **27**, 61–71.
20 J. Gandhi, K. Godse and G. Godse, *Indian J. Drugs Dermatol.*, 2018, **4**, 3.
21 A. Noor, N. G. Qazi, H. Nadeem, A.-U. Khan, R. Z. Paracha, F. Ali and A. Saeed, *Chem. Cent. J.*, 2017, **11**, 85.
22 Z. Wu, M.-B. Xia, D. Bertsetseg, Y.-H. Wang, X.-L. Bao, W.-B. Zhu, P.-R. Chen, H.-S. Tang, Y.-J. Yan and Z.-L. Chen, *Bioorg. Chem.*, 2020, 104042.
23 M. Rashid, *Bioorg. Chem.*, 2020, **96**, 103576.
24 M. Taha, A. Mosaddik, F. Rahim, S. Ali, M. Ibrahim and N. B. Almandil, *J. King Saud Univ., Sci.*, 2020, **32**, 191–194.
25 G. Navarrete-Vázquez, H. Moreno-Diaz, F. Aguirre-Crespo, I. Leon-Rivera, R. Villalobos-Molina, O. Munoz-Muniz and S. Estrada-Soto, *Bioorg. Med. Chem. Lett.*, 2006, **16**, 4169–4173.
26 P. Vasil'ev, K. Y. Kalitin, A. Spasov, O. Y. Grechko, V. Poroikov, D. Filimonov and V. Anisimova, *Pharm. Chem. J.*, 2017, **50**, 775–780.
27 A. Rathore, R. Sudhakar, M. J. Ahsan, A. Ali, N. Subbarao, S. S. Jadav, S. Umar and M. S. Yar, *Bioorg. Chem.*, 2017, **70**, 107–117.
28 R. Vinodkumar, S. D. Vaidya, B. V. S. Kumar, U. N. Bhise, S. B. Bhirud and U. C. Mashelkar, *Eur. J. Med. Chem.*, 2008, **43**, 986–995.
29 P. Saha, S. R. Brishty and S. A. Rahman, *Indian J. Pharm. Sci.*, 2020, **82**, 222–229.
30 R. Walia, M. Hedaitullah, S. F. Naaz, K. Iqbal and H. Lamba, *Int. J. Res. Pharm. Chem.*, 2011, **1**, 565–574.
31 M. Shaharyar and A. Mazumder, *Arabian J. Chem.*, 2017, **10**, S157–S173.
32 B. Goswami and A. K. Singh, *Int. J. Sci. Innovs.*, 2012, **2**, 121–136.
33 S. Neidle, *Biopolymers*, 1997, **44**, 105–121.
34 T. L. Huang, B. Tao, Y. Quarshie, S. F. Queener and I. O. Donkor, *Bioorg. Med. Chem. Lett.*, 2001, **11**, 2679–2681.
35 C. A. Bell, M. Cory, T. Fairley, J. Hall and R. Tidwell, *Antimicrob. Agents Chemother.*, 1991, **35**, 1099–1107.
36 M. Cory, R. Tidwell and T. Fairley, *J. Med. Chem.*, 1992, **35**, 4767.
37 R. R. Tidwell, S. K. Jones, N. A. Naiman, L. C. Berger, W. B. Brake, C. C. Dykstra and J. E. Hall, *Antimicrob. Agents Chemother.*, 1993, **37**, 1713–1716.
38 T. A. Fairley, R. R. Tidwell, I. Donkor, N. A. Naiman, K. A. Ohemeng, R. J. Lombardy, J. A. Bentley and M. Cory, *J. Med. Chem.*, 1993, **36**, 1746–1753.
39 H. Goker, M. Alp and S. Yildiz, *Molecules*, 2005, **10**, 1377–1386.
40 H. Goker, S. Ozden, S. Yildiz and D. W. Boykin, *Eur. J. Med. Chem.*, 2005, **40**, 1062–1069.
41 S. Ozden, D. Atabey, S. Yildiz and H. Goker, *Bioorg. Med. Chem.*, 2005, **13**, 1587–1597.
42 M. O. Puskullu, S. Yildiz, Y. Duydu, A. Ustundag and H. Goker, *J. Enzyme Inhib. Med. Chem.*, 2015, **30**, 173–179.
43 Z. Ates-Alagöz, M. Alp, C. Kus, S. Yildiz, E. Buyukbingöl and H. Göker, *Arch. Pharm.*, 2006, **339**, 74–80.
44 C. Karaaslan, *Turk. J. Pharm. Sci.*, 2020, **17**, 108.
45 K. Starčević, M. Kralj, K. Ester, I. Sabol, M. Grce, K. Pavelić and G. Karminski-Zamola, *Bioorg. Med. Chem.*, 2007, **15**, 4419–4426.
46 M. Alp, H. Göker, R. Brun and S. Yıldız, *Eur. J. Med. Chem.*, 2009, **44**, 2002–2008.
47 S. Özden, D. Atabey, S. Yıldız and H. Göker, *Bioorg. Med. Chem.*, 2005, **13**, 1587–1597.
48 M. O. Püsküllü, S. Yıldız, Y. Duydu, A. Üstündağ and H. Göker, *J. Enzyme Inhib. Med. Chem.*, 2015, **30**, 173–179.
49 H. Karataş, M. Alp, S. Yıldız and H. Göker, *Chem. Biol. Drug Des.*, 2012, **80**, 237–244.
50 H. Göker, M. Tunçbilek, S. Süzen, C. Kus and N. Altanlar, *Arch. Pharm.*, 2001, **334**, 148–152.
51 M. Erol, I. Celik, O. Temiz-Arpaci, H. Goker, F. Kaynak-Onurdag and S. Okten, *Med. Chem. Res.*, 2020, 1–11.
52 P. Wayne, *Performance standards for antimicrobial susceptibility testing*, 18th informational supplement, M100-S18, Clinical and Laboratory Standards Institute, 2018.
53 A. S. S. Edition, CLSI document H3-A6.
54 L. Schrödinger, Maestro, Schrödinger, LLC, New York, NY, 2018.
55 S. I. Qureshi and H. K. Chaudhari, *Bioorg. Med. Chem.*, 2019, **27**, 2676–2688.
56 R. Bouley, M. Kumarasiri, Z. Peng, L. H. Otero, W. Song, M. A. Suckow, V. A. Schroeder, W. R. Wolter, E. Lastochkin and N. T. Antunes, *J. Am. Chem. Soc.*, 2015, **137**, 1738–1741.
57 I. Celik, M. Erol, O. T. Arpaci, F. S. Senol and I. E. Orhan, *Polycyclic Aromat. Compd.*, 2020, 1–12.

58 S. Genheden and U. Ryde, *Expert Opin. Drug Discovery*, 2015, **10**, 449–461.
59 N. Chadha, A. K. Tiwari, V. Kumar, S. Lal, M. D. Milton and A. K. Mishra, *J. Biomol. Struct. Dyn.*, 2015, **33**, 978–990.
60 M. Frisch, G. Trucks, H. Schlegel, G. Scuseria, M. Robb, J. Cheeseman, G. Scalmani, V. Barone, B. Mennucci and G. Petersson, There is no corresponding record for this reference, 2015.
61 A. Hellal, S. Chafaa, N. Chafai and L. Touafri, *J. Mol. Struct.*, 2017, **1134**, 217–225.
62 K. Benbouguerra, S. Chafaa, N. Chafai, M. Mehri, O. Moumeni and A. Hellal, *J. Mol. Struct.*, 2018, **1157**, 165–176.
63 M. Djenane, S. Chafaa, N. Chafai, R. Kerkour and A. Hellal, *J. Mol. Struct.*, 2019, **1175**, 398–413.
64 N. Chafai, S. Chafaa, K. Benbouguerra, A. Hellal and M. Mehri, *J. Mol. Struct.*, 2019, **1181**, 83–92.
65 M. Mehri, N. Chafai, L. Ouksel, K. Benbouguerra, A. Hellal and S. Chafaa, *J. Mol. Struct.*, 2018, **1171**, 179–189.
66 N. Chafai, S. Chafaa, K. Benbouguerra, D. Daoud, A. Hellal and M. Mehri, *J. Taiwan Inst. Chem. Eng.*, 2017, **70**, 331–344.
67 R. K. Tittal, P. Yadav, K. Lal and A. Kumar, *New J. Chem.*, 2019, **43**, 8052–8058.
68 S. Celik, F. Ozkok, A. E. Ozel, Y. Müge Sahin, S. Akyuz, B. D. Sigirci, B. B. Kahraman, H. Darici and E. Karaoz, *J. Biomol. Struct. Dyn.*, 2019, 1–15.
69 T. Roy Dennington and J. M. Millam, *GaussView, Version 6.0*, 2016.
70 L. Llorach-Pares, A. Nonell-Canals, C. Avila and M. Sanchez-Martinez, *Mar. Drugs*, 2018, **16**, 386.
71 S. Release, Qikprop, Schrödinger, LLC, New York, NY, 2018.
72 H. Göker, M. Alp and S. Yıldız, *Molecules*, 2005, **10**, 1377–1386.
73 M. O. Puskullu, I. Celik, M. Erol, H. Fatullayev, E. Uzunhisarcikli and G. Kuyucuklu, *Bioorg. Chem.*, 2020, 104014.
74 V. R. Mishra, C. W. Ghanavatkar, S. N. Mali, H. K. Chaudhari and N. Sekar, *J. Biomol. Struct. Dyn.*, 2020, **38**, 1772–1785.
75 S. Parveen, F. Arjmand, Q. Zhang, M. Ahmad, A. Khan and L. Toupet, *J. Biomol. Struct. Dyn.*, 2020, 1–17.
76 Y. S. Mary, G. Yalcin, Y. S. Mary, K. Resmi, R. Thomas, T. Önkol, E. N. Kasap and I. Yildiz, *Chem. Pap.*, 2020, 1–8.
77 S. Beegum, C. Y. Panicker, S. Armaković, S. J. Armaković, M. Arisoy, O. Temiz-Arpaci and C. Van Alsenoy, *J. Mol. Struct.*, 2019, **1176**, 881–894.
78 S. Shahab, M. Sheikhi, L. Filippovich, R. Kumar, E. Dikusar, H. Yahyaei and M. Khaleghian, *J. Mol. Struct.*, 2017, **1148**, 134–149.
79 S. H. Lone, S. Jameel, M. A. Bhat, R. A. Lone, R. J. Butcher and K. A. Bhat, *RSC Adv.*, 2018, **8**, 8259–8268.
80 M. S. Almutairi, A. S. Zakaria, P. P. Ignasius, R. I. Al-Wabli, I. H. Joe and M. I. Attia, *J. Mol. Struct.*, 2018, **1153**, 333–345.